Improvement of power quality using a robust hybrid series active power filter

Sushree Diptimayee Swain, Pravat Kumar Ray, *Member, IEEE* and Kanungo Barada Mohanty, *Senior Member, IEEE*

***Abstract*—The degradation in power quality causes adverse economical impact on the utilities and customers. Harmonics in current and voltage are one of the most commonly known power quality issues and are solved by the use of hybrid series active power filter (HSAPF) . In this paper, a new controller design using sliding mode controller-2 is proposed to make the HSAPF more robust and stable. An accurate averaged model of three-phase HSAPF is also derived in this paper. The design concept of the robust HSAPF has been verified through simulation and experimental studies and the results obtained are discussed.**

***Index Terms*—Robust HSAPF, sliding mode controller, power quality, hybrid active power filter, averaged model.**

I. Introduction

Over the past few years, the enormous increase in the use of non-linear loads, arises many power quality issues like high current harmonics, voltage distortion and low power factor etc. on electrical grid [1]. Hence the proliferation of non-linear load in system generates harmonic currents injecting into the AC power lines. This distorted supply voltage and current causes malfunction of some protection devices, burning of transformers and motors, overheating of cables. Hence it is most important to install compensating devices for the compensation of harmonic currents and voltages produced due to non-linear load. Traditionally, passive power filters have been used as a compensating device, to compensate distortion generated by constant non-linear loads. These filters [2] are designed to provide a low impedance path for harmonics and maintaining good power quality with an simplest design and low cost. However, passive filters have some demerits like mistuning, resonance, dependence on the conditions of the power supply system and large values of passive component that leading to bulky implementations.

Sushree Diptimayee Swain, Pravat Kumar Ray and Kanungo Barada Mohanty are working in the Department of Electrical Engineering, National Institute of Technology, Rourkela-769 008, India. Email:sushreedipti@gmail.com, rayp@nitrkl.ac.in, kbmohanty@nitrkl.ac.in

For high-quality power requirements, numerous topologies of active filters i.e. APF connected in series or in parallel (series active filters and shunt active filters) to the nonlinear loads with the aim of improving voltage or current distortion. These filters are the most widely used solution, as they efficiently eliminate current distortion and the reactive power produced by non-linear loads. But they are generally expensive and have high operating losses [3] [4]. Henceforth to overcome these drawbacks and to improve the compensation performance with reduced cost of the APFs, a novel HAPF topology-III is introduced by Peng et al. in 1988 [5], in which APF is connected in series with the source as well as non-linear load and PPF connected in parallel with the load, which behaves as power factor correction capacitor is proposed. This topology [6] attracted much more attention to endure high load currents and works as a harmonic isolator between source and non-linear load.

The control strategy is important to enhance the performance of HSAPF. In reality, many articles for hybrid power filter have already proposed advanced techniques to reduce current harmonics created by these non-linear loads. In [7], a linear feedback-feed-forward controller is designed for hybrid power filter. But this controller is not easy for getting both steady-state and transient state performances with the linear control strategy because the dynamic model of HSAPF system contains multiplication terms of control inputs and state variables. Due to the non-linear characteristics of HSAPF, a sliding mode controller is presented in [8]. The sliding mode control is known as an appropriate control technique for controlling non-linear systems with uncertain dynamics and disturbances due to its order reduction property and low sensitivity to disturbances and plant parameter variations, which reduces the burden of the requirement of exact modeling. Furthermore, this sliding mode control also diminishes the complicacy of feedback control design by means of decoupling the system into individual subsystems of lower dimension. Because of these given properties, the implementation of sliding mode control can be found in the areas of power electronic switching devices. The principle of

sliding mode control is defined as to enforce the sliding mode motion in a predefined switching surfaces of the system state space using discontinuous control. The switching surfaces should be selected in such a way that sliding motion would maintain desired dynamics of motion according to certain performance criterion. The conventional control methods, such as Linear-quadratic regulator (LQR) [9] or Linear quadratic Gaussian (LQG) servo controller [10] for linear systems, are required to choose proper switching surfaces. Then, the discontinuous control needs to be chosen such that any states outside of the discontinuity surface are enforced to reach the surface at finite time. Accordingly, sliding mode occurs along the surface, and the system follows the desired system dynamics.

The main difficulty of hardware implementation of classical sliding mode control method is chattering. Chattering is nothing but an undesirable phenomenon of oscillation with finite frequency and amplitude. The chattering is dangerous because the system lags control accuracy, high wear of moving mechanical parts, and high heat losses occurs in electrical power circuits. Chattering occurs because of unmodeled dynamics. These unmodeled dynamics are created from servomechanisms, sensors and data processors with smaller time constants. In sliding mode control the switching frequency should be considerably high enough to make the controller more robust, stable and no chattering because chattering reduces if switching frequency of the system increases. The application of sliding mode controller in power converter systems for example in HSAPF, a natural way to reduce chattering is increasing switching frequency. However, it is not possible in case of power converters because of certain limitations in switching frequency for losses in power converters, for which it results in chattering. Therefore, this chattering problem cannot blame sliding mode implementation since it is mainly caused by switching limitations. In [11], it is shown that the chattering exponentially tends to zero if the relative degree of the system with actuators or sensors is two. The relative degree of HSAPF system is two. Because of this relative degree of HSAPF system and also for these obstacles in classical sliding mode controller, this research paper proposed a new controller i.e. sliding mode controller-2. This proposed controller suppressed chattering and enhance the performance of HSAPF. This controller is completely new for this topology of HSAPF system. The recent research paper [12] focuses on carrier based PWM (CBPWM) for HSAPF topology. But in some cases the CBPWM based HSAPF may not be completely measurable in most of the real-world situations. In case of CBPWM, power system perturbations have not been taken into consideration and also the presence of a time delay at the reference tracking point gives rise to a slow response of the overall system. Thus, tracking error is not reduced effectively and stability of the system is minimally improved. To overcome this, a SMC-2 controller is proposed for voltage source converter (VSC). The idea behind this controller is to achieve gain stability, perfect tracking and distortion free current and load voltage. In view of above mentioned issues, we give more emphasis on the development of robust controller with a faster reference tracking approach in HSAPF, which permits all perturbations such as load voltage distortion, parametric variation of load, source current distortion and supply voltage unbalance so that compensation capability of the HSAPF system can be enhanced.

This paper is organized as follows. In section II, the description of schematic of system topology and hardware modules of three phase HSAPF model is explained. Section-III depicts the averaged modelling of HSAPF system. Section-IV disclose the controller design for HSAPF. Section-V depicts the simulation as well as experimental results for harmonic compensation using HSAPF. Section-VI presents the conclusions of this work.

II. Description of schematic of system topology and hardware modules of HSAPF model

Fig. 1 and Fig. 2 demonstrates the experimental prototype and schematic diagram of hybrid series active power filter (HSAPF) developed in the laboratory. This topology of HSAPF is composed of a series connected active power filter (SAPF) and a shunt connected passive power filter (PPF). PPF connected in parallel with the load. The PPF consists of fifth, seventh tuned LC filter of rating (L_{pf}= 1.86mH and C_{pf}= 60μF) for the compensation of harmonic current on load side. The SAPF connected in series with the source through a matching transformer of turn ratio 1:2 to ensure galvanic isolation. SAPF consists of three parts such as:-three phase IGBT based SEMIKRON inverter, a DC-link capacitor of 2200μF and a three phase high frequency LC filter of impedances (C_f= 60μF, L_f= $1.35mH$). The high frequency LC filter is applied to get rid of high frequency switching ripples from the compensating voltage supplied by the inverter. A non-linear load comprising of a three phase diode bridge rectifier (SQL 100V 100A) with RL-load (i.e.resistor of $8.5A$, 100Ω and inductor of $40mH$) is considered. There are 7 no. of voltage sensors (LEM LV 25-P) and 3 no. of current sensors (LEM LA 55-P) mandatory. Sensors sense voltages, currents and given its input to the dSPACE 1103 R and D board. The control

This article has been accepted for publication in a future issue of this journal, but has not been fully edited. Content may change prior to final publication. Citation information: DOI 10.1109/TPEL.2016.2586525, IEEE Transactions on Power Electronics

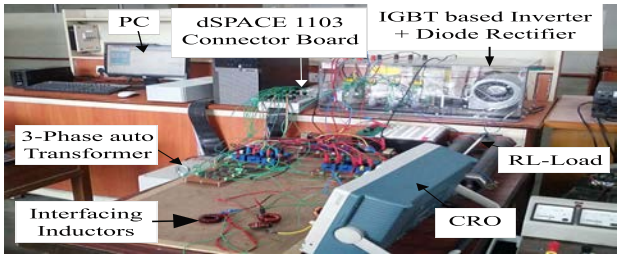

(a)

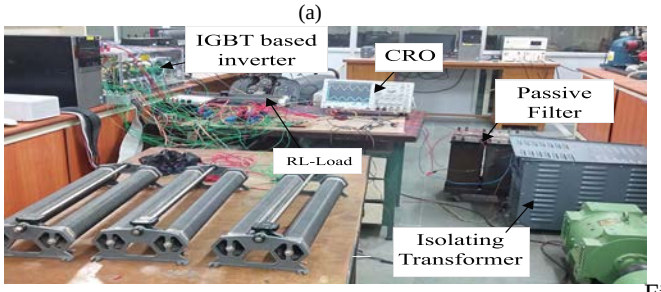

(b)

Fig. 1: (a) Experimental Setup of SAPF. (b) Experimental Setup of HSAPF

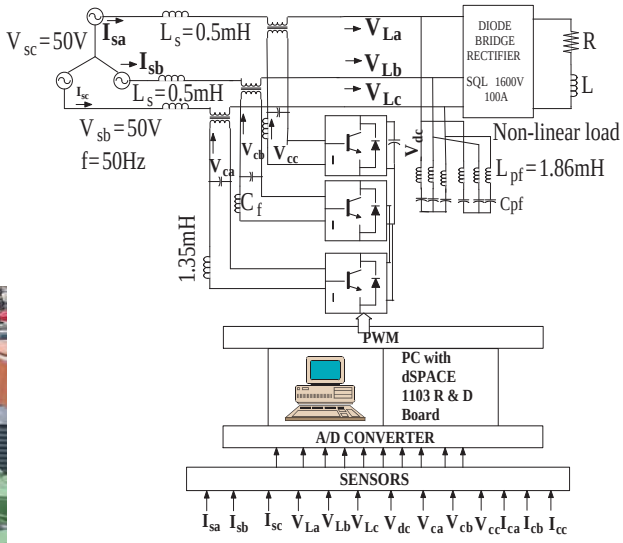

Fig. 2: Schematic diagram of the control and power circuit of HSAPF.

of HSAPF is achieved by controller based algorithm implemented with dSPACE 1103. At first, the controller is implemented using MATLAB/Simulink. The real time workshop is used to produce C code for real time applications. The interface between MATLAB/ Simulink and dSPACE 1103 permit running the control algorithm. The basic control structure and its mathematical equations are presented in section-IV. The switching signals are generated from the slave DSP. The generated switching pulse used as input to the amplifier circuit. The function of amplifier circuit is to convert 5V to 15V. The amplifier circuit consists of CD4504 and an isolating circuit of HCPL 2601. The output of amplifier circuit behaved as input to the driver of inverter. For implementation, the control algorithm at a fixed step size of $100\mu s$ and hence, the maximum switching frequency of PWMVSI of HSAPF is fixed at 10kHz. The design specifications and circuit parameters in laboratory prototype are given in Table I.

III. Averaged Modelling of HSAPF

Fig. 2 shows the schematic diagram of the control and power circuit of 3-phase HSAPF. The SAPF consists of a voltage source inverter connected to the grid through an LC filter and a three phase linear transformer. The series resistance of the inductors are neglected. Where, u_a, u_b and u_c are the duty cycle of the inverter legs in a switching period, whereas V_{ca}, V_{cb}, V_{cc} are the output voltage of series active filter for three phases are shown in Fig. 2 and I_{ca}, I_{cb}, I_{cc} are known as the three phase current output of active filter, V_{aN}, V_{bN}, V_{cN} are the phase voltages for three phases, I_{sa}, I_{sb}, I_{sc} are known as the three phase source current, V_{nN} is the neutral voltage. By averaging the inverter legs in the circuit diagram, the whole averaged model [13] of the inverter in three phases are obtained as shown in Fig. 3. From this circuit diagram, the dynamic model of HSAPF under synchronous reference frame can be expressed by the following differential equations:

$$\frac{di_{cd}}{dt} = \frac{V_{cd}}{L_f} + wi_{cq} - \frac{u_d V_{dc}}{L_f} \tag{1}$$

$$\frac{di_{cq}}{dt} = \frac{V_{cq}}{L_f} - wi_{cd} - \frac{u_q V_{dc}}{L_f} \tag{2}$$

$$\frac{dV_{cd}}{dt} = wV_{cq} - \frac{i_{cd}}{C_f} + \frac{i_{sd}}{C_f} \tag{3}$$

$$\frac{dV_{cq}}{dt} = -wV_{cd} - \frac{i_{cq}}{C_f} + \frac{i_{sq}}{C_f} \tag{4}$$

$$\frac{dV_{dc}}{dt} = \frac{3}{2C_{dc}}\left(u_d i_{cd} + u_q i_{cq}\right) \tag{5}$$

Where, V_{cd} and V_{cq} are the dq-axis compensating voltages, u_d and u_q are the dq-axis duty ratio, ω is the angular frequency of the source voltage. To facilitate the controller design, the HSAPF system model can be defined as follows:

$$\begin{cases} x^{\cdot} = f(x) + g(x)\,u \\ y = h(x) \end{cases} \tag{6}$$

Where $x = [i_{cd}, i_{cq}, V_{cd}, V_{cq}, V_{dc}]^T$ is defined as the state vector, vector $u = [u_d, u_q]^T$ stands for system control variables, vector $y = [y_1, y_2]^T = [V_{cd}, V_{cq}]^T$ presents the system outputs. It must be noticed that the achieved multi-input multi-output(MIMO) system is non-linear because of existence of multiplication terms of the state variables and control variables. And also the state variables are intensely combined to each other.

This article has been accepted for publication in a future issue of this journal, but has not been fully edited. Content may change prior to final publication. Citation information: DOI 10.1109/TPEL.2016.2586525, IEEE Transactions on Power Electronics

These two difficulties can be accurately controlled by the design of sliding mode controller, which openly examine the link between the control variables and the system outputs.

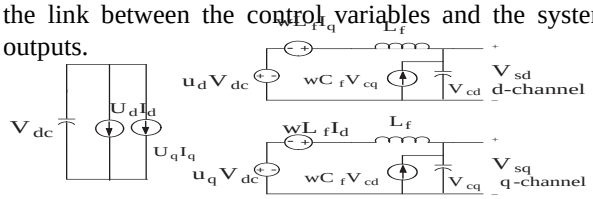

Fig. 3: Averaged equivalent circuit in three phase stationary frame of HSAPF

IV. Development of the Control System

A. Reference voltage generation scheme (Hybrid control approach based synchronous reference frame method (HSRF))

The reference compensation voltage of the HSAPF system adopting hybrid control approach based synchronous reference frame method are expressed as:

$$V_c^* = KI_{sh} - V_{Lh} \tag{7}$$

This hybrid control approach simultaneously detect both source current I_s as well as load voltage V_L to obtain their harmonic components. The generation of reference compensating signal V_c^* using the combined load voltage and source current detection scheme together with adopting hybrid control approach based synchronous reference frame method for HSAPF system can be obtained as (8) and (9). The realization circuit for generating V_c^* is shown in Fig. 4

$$U_d = KI_d - V_d \tag{8}$$

$$U_q = KI_q - V_q \tag{9}$$

The generation of reference compensating signal using the combined load voltage and source current detection scheme [14] is shown in Fig. 4. From Fig. 4, the error between the reference and the actual DC-link voltage of DC-link capacitor of three phase PWM inverter fed from the ac system is first passed through a PI controller and then it is subtracted from the oscillatory component in d-axis. Since the extra fundamental components are added to harmonic components respectively. Thus the reference compensating voltages are also expressed as:

$$\left.\begin{aligned} V_{ca}^* &= KI_{sah} - V_{Lah} + \Delta V_{caf} \\ V_{cb}^* &= KI_{sbh} - V_{Lbh} + \Delta V_{cbf} \\ V_{cc}^* &= KI_{sch} - V_{Lch} + \Delta V_{ccf} \end{aligned}\right\} \tag{10}$$

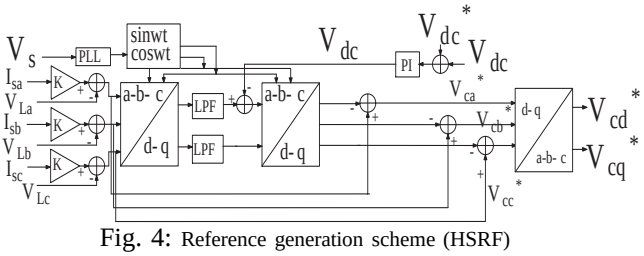

Fig. 4: Reference generation scheme (HSRF)

B. Proposed sliding mode controller design for HSAPF

This section describes the synthesis of sliding mode controller based on the averaged model of HSAPF system. Based on system model (6), we differentiate the compensating voltage with respect to time until the control variables u_d and u_q appear explicitly, which leads the following equations as:

$$\frac{dV_{cd}}{dt} = wV_{cq} - \frac{i_{cd}}{C_f} + \frac{i_{sd}}{C_f} \tag{11}$$

$$\frac{dV_{cq}}{dt} = -wV_{cd} - \frac{i_{cq}}{C_f} + \frac{i_{sq}}{C_f} \tag{12}$$

$$\begin{aligned} \frac{d^2V_{cd}}{dt^2} = -w^2V_{cd} - w\frac{i_{cq}}{C_f} + w\frac{i_{sq}}{C_f} - \frac{V_{cd}}{L_fC_f} \\ -w\frac{i_{cq}}{C_f} - \frac{u_dV_{dc}}{L_fC_f} + \frac{di_{sd}}{dt}\cdot\frac{1}{C_f} \end{aligned} \tag{13}$$

$$\begin{aligned} \frac{d^2V_{cq}}{dt^2} = -w^2V_{cq} - w\frac{i_{cd}}{C_f} + w\frac{i_{sd}}{C_f} - \frac{V_{cq}}{L_fC_f} \\ -w\frac{i_{cd}}{C_f} - \frac{u_qV_{dc}}{L_fC_f} + \frac{di_{sq}}{dt}\cdot\frac{1}{C_f} \end{aligned} \tag{14}$$

So the relative degree of the system is '2' because at 2nd derivative of compensating voltage in dq-axis we get control variables u_d and u_q. The Jacobi matrix of $j\,(d)$ with respect to the control vector $'u'$ can be calculated as follows:

$$\frac{\partial j(d)}{\partial d^T} = \begin{bmatrix} \frac{-V_{dc}}{L_f} & 0 \\ 0 & \frac{-V_{dc}}{L_f} \end{bmatrix} \tag{15}$$

In fact, the dc-link voltage V_{dc} is positive in the operating range. $\frac{\partial j(d)}{\partial d^T}$ is non-singular. Henceforth the relative degree vector of system is $\beta = [\beta_1, \beta_2]^T = [2, 2]^T$ and $\beta_1 + \beta_2 = 2 + 2 = 4$ is strictly less than the system order $n = 5$. To synthesize a robust HSAPF system, a sliding mode controller is designed based on the linearised model (6). The control objective of the HSAPF system is to force the compensating voltages V_{cd} and V_{cq} , the mathematical expression of sliding surface as follows:

$$\overline{S} = \begin{bmatrix} \overline{S}_d \\ \overline{S}_q \end{bmatrix} \tag{16}$$

$$\overline{S} = S + \alpha\,\dot{S} \tag{17}$$

$$\overline{S}_d = S_d + \dot{S}_d \tag{18}$$

$$\overline{S}_q = S_q + \dot{S}_q \tag{19}$$

putting the values of V_{cd} and V_{cq} in (20) and (22)

$$\overline{S}_d = (V_{cd} - V_{cd}^*) + \alpha_1\left(\dot{V_{cd}} - \dot{V_{cd}}^*\right) \tag{20}$$

$$\dot{\overline{S}}_d = \left(\dot{V_{cd}} - \dot{V_{cd}}^*\right) + \alpha_1\left(\ddot{V_{cd}} - \ddot{V_{cd}}^*\right) \tag{21}$$

$$\overline{S}_q = (V_{cq} - V_{cq}{}^*) + \alpha_2 \left(\dot{V_{cq}} - \dot{V_{cq}}{}^* \right) \quad (22)$$

$$\dot{\overline{S}}_q = \left(\dot{V_{cq}} - \dot{V_{cq}}{}^* \right) + \alpha_2 \left(\dot{V_{cq}} - \dot{V_{cq}}{}^* \right) \quad (23)$$

Where α is a positive constant The design procedure of sliding mode controller is depicted as:

$$\dot{\overline{S}} = 0 \quad (24)$$

$$\dot{\overline{S}}_d = 0 \quad (25)$$

substituting (11) and (13) in (25), the equivalent control law in d-axis can be directly derived as:

$$U_{deqv.} = -\left(\dot{V_{cd}^*} + \alpha \ddot{V_{cd}^*} \right) + \frac{L_f}{V_{dc}} \left(C_f w V_{cq} - i_{cd} + i_{sd} \right) + \frac{\alpha L_f}{V_{dc}} \left(-C_f w^2 V_{cd} - w i_{cq} + w i_{sq} - \frac{V_{cd}}{L_f} - w i_{cq} + \dot{i_{sd}} \right) \quad (26)$$

Similarly, equivalent control law in q-axis has been derived as follows

$$U_{qeqv.} = -\left(\dot{V_{cq}^*} + \alpha \ddot{V_{cq}^*} \right) + \frac{L_f}{V_{dc}} \left(C_f w V_{cd} - i_{cq} + i_{sq} \right) + \frac{\alpha L_f}{V_{dc}} \left(-C_f w^2 V_{cq} - w i_{cd} + w i_{sd} - \frac{V_{cq}}{L_f} - w i_{cd} + \dot{i_{sq}} \right) \quad (27)$$

$$U = U_{eqv.} + U_{switching} \quad (28)$$

$$U_d = U_{deqv.} + U_{dswitching} \quad (29)$$

$$U_q = U_{qeqv.} + U_{qswitching} \quad (30)$$

The non-linear control law has been directly derived on putting the values of $U_{deqv.}$, $U_{qeqv.}$ in (29) and (30).

$$U_d = -\left(\dot{V_{cd}^*} + \alpha \ddot{V_{cd}^*} \right) + \frac{L_f}{V_{dc}} \left(C_f w V_{cq} - i_{cd} + i_{sd} \right) + \frac{\alpha L_f}{V_{dc}} \left(-C_f w^2 V_{cd} - w i_{cq} + w i_{sq} - \frac{V_{cd}}{L_f} - w i_{cq} + \dot{i_{sd}} \right) - K_{11} sign\left(S_d\right) - K_{12} sign\left(\dot{S_d}\right) \quad (31)$$

$$U_q = -\left(\dot{V_{cq}^*} + \alpha \ddot{V_{cq}^*} \right) + \frac{L_f}{V_{dc}} \left(C_f w V_{cd} - i_{cq} + i_{sq} \right) + \frac{\alpha L_f}{V_{dc}} \left(-C_f w^2 V_{cq} - w i_{cd} + w i_{sd} - \frac{V_{cq}}{L_f} - w i_{cd} + \dot{i_{sq}} \right) - K_{21} sign\left(S_q\right) - K_{22} sign\left(\dot{S_q}\right) \quad (32)$$

The control block diagram of the proposed control strategy has been illustrated in Fig. 5

The Control function of this controller is as follows:

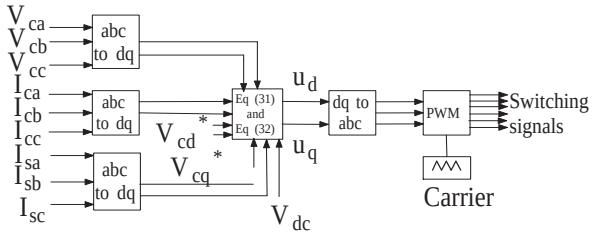

Fig. 5: Proposed sliding mode control structure for HSAPF

$U_{eq} = U_{switching}$

$$U_{eq} = \begin{cases} +1, WhenS > 0 \\ -1, WhenS < 0 \end{cases} \quad (33)$$

For the satisfactory operation of HSAPF system, this controller meets stability condition.

C. Stability analysis of sliding mode controller based HSAPF

This segment analyzes the stability of the HSAPF system with the suggested control strategy. For the stability analysis of the system external dynamics of V_{cd} and V_{cq}, we define a sliding manifold as follows:

$$\overline{S} = \begin{bmatrix} \overline{S}_d & \overline{S}_q \end{bmatrix}^T = 0 \quad (34)$$

For the evidence of system stability with the sliding mode controller, we adopt a Lyapunov function as a candidate function i.e.

$$V(x) = \frac{1}{2} \overline{S}^T \overline{S} \quad (35)$$

whose time derivative is

$$\dot{V} = \begin{bmatrix} \overline{S}_d & \overline{S}_q \end{bmatrix} \begin{bmatrix} \dot{\overline{S}}_d \\ \dot{\overline{S}}_q \end{bmatrix} \quad (36)$$

substituting (20) to (23) in (36), we can get

$$\dot{V} = -S_d \left(\frac{i_{cd}}{C_f} - \frac{i_{sd}}{C_f} - w V_{cq} + \dot{V_{cd}^*} \right) - S_d \alpha_1 \left(-K_{11} sign\left(S_d\right) - K_{12} sign\left(\dot{S_d}\right) - \dot{V_{cd}^*} \right) - S_q \left(\frac{i_{cq}}{C_f} - \frac{i_{sq}}{C_f} - w V_{cd} + \dot{V_{cd}^*} \right) - S_q \alpha_2 \left(-K_{21} sign\left(S_q\right) - K_{12} sign\left(\dot{S_q}\right) - \dot{V_{cq}^*} \right) \quad (37)$$

We can see from (37) that $\dot{V}(x) \leqslant 0$, If in a region, there exist a scalar function $V(x)$ with continuous first partial derivatives such that

-$V(x)$ is positive definite

-$\dot{V}(x)$ is negative semi-definite

Then the equilibrium point is stable. If, actually, the derivative $\dot{V}(x)$ is locally negative definite in exist

This article has been accepted for publication in a future issue of this journal, but has not been fully edited. Content may change prior to final publication. Citation information: DOI 10.1109/TPEL.2016.2586525, IEEE Transactions on Power Electronics

region, then the system is stable. Which means the attractiveness of the manifold (34) is stable for proposed sliding mode controller-2 based HSAPF.

In this proposed control approach the control signal satisfies all the above conditions, so that the state trajectories are moved towards the switching surface. Henceforth during the operation of this proposed controller, the HSAPF system achieves fast response, good robustness and throwaway disturbances effectively.

V. Results and Discussions

A. Simulation results

The reference generation approach (HSRF method) with the switching pattern generation scheme (i.e. sliding mode controller-2) of HSAPF system given in Fig. 2 is tested using MATLAB/Simulink software. A 3-phase source voltage is applied to a harmonic voltage producing non-linear load. This voltage producing non-linear load comprises of a 3-phase diode bridge rectifier feeding an RL-load. Due to this type of non-linear load, a harmonic distortion occurs in both source current as well as in load voltage. This harmonic contamination are the reasons of power quality disturbances. So power quality disturbances can be eradicated by means of HSAPF. The simulation as well as experimental parameters are encapsulated in Table-I. One reference generation technique and one modulation technique, i.e. hybrid control approach based SRF method (HSRF) and sliding mode controller based HSAPF are verified and analyzed using the following MATLAB simulation results. In order to verify the reliability of the proposed controller, the system is simulated under MATLAB/Simulink version 2010. The goal of simulation is to reduce the THD response of sliding mode controller based HSAPF below 5%. And also a HSRF combined with sliding mode controller technique utilizes DC-link voltage properly for equivalent control law generation. MATLAB simulation results for source voltage V_s, load current I_L, source current I_s, dc voltage V_{dc} for steady state as well as dynamic condition of load under existing method has been presented in Fig. 6. The nature of the source current without filter is exactly like load current. MATLAB simulation results for source voltage V_s, load current I_L, source current I_s, dc voltage V_{dc} for steady state, dynamic condition of load, parametric variation of HSAPF system under sliding mode controller-2 has been depicted in Fig. 7 and Fig. 8 respectively. From the simulation results, it is proved that the THD response of sliding mode controller based HSAPF is smaller than the THD response of existing technique based HSAPF. Simulation results under several system operating conditions of load have verified the design concept of the suggested highly effective and robust sliding mode based HSAPF. The robustness of the proposed HSAPF has been analyzed here. In proposed controller the source current THD is reduced from 20.14% to 1.62%. For transient condition of load, the THD of source current for the proposed controller based HSAPF is reduced from 26.7% to 2.16%. The harmonic compensation Ratio (HCR) for steady state, parametric variation of HSAPF system case are approximately same but the HCR in transient case of non-linear load is differed by only 0.55% from the above two cases. Thus, the THDs of the source current are unaffected by the parametric variations of load. This proves the robustness of the proposed HSAPF under parametric variations of load. The HCR factor is calculated as follows:

$$HCR = \frac{THD(\%)AfterCompensation}{THD(\%)BeforeCompensation} * 100\%$$

TABLE I: System Parameters Used for Simulation and Experiment

Line voltage and frequency	$V_s = 50V(RMS)$, f=50Hz
Line impedance	$L_s = 0.5mH$, $R_s = 0.1\Omega$
Non-linear load impedance	L=40mH, $R = 100\Omega$, 8.5A
Series active filter parameter	$C_f = 60\mu F$, $L_f = 1.35mH$, $C_{dc} = 2200\mu F$, $V_{dc} = 40V$
Shunt passive filter parameter	$L_{pf} = 1.86mH$, $C_{pf} = 60\mu F$

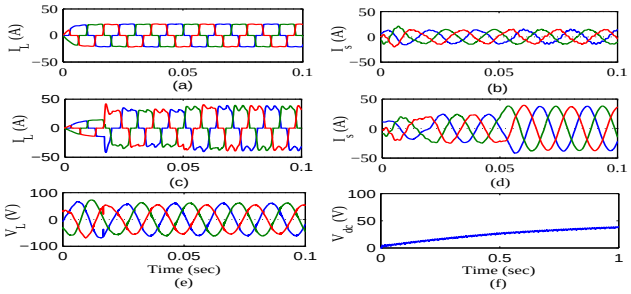

Fig. 6: (a) Steady state response of load current before compensation (b) Steady state response of source current after compensation (c) Transient response of load current before compensation (d) Transient response of source current after compensation (e) Load voltage after compensation (f) DC-link voltage for existing method (ideal sliding mode controller)

B. Experimental Results

The proposed control algorithm has been implemented in real time on the hardware setup developed in our laboratory. A prototype of the experimental setup is shown in Fig. 1. The efficacy of the proposed scheme is compared with the existing method [15](Harmonic series compensators in power systems: their control via sliding mode), in which instantaneous reactive power theory used as reference generation process and ideal sliding mode controller with carrier based PWM is applied for switching pattern generation. The demerit of this controller is switching frequency i.e. it require high

This article has been accepted for publication in a future issue of this journal, but has not been fully edited. Content may change prior to final publication. Citation information: DOI 10.1109/TPEL.2016.2586525, IEEE Transactions on Power Electronics

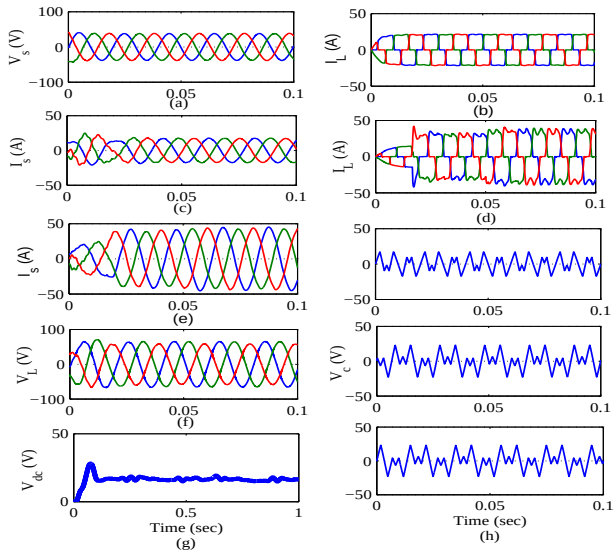

Fig. 7: (a) Source voltage (b) Steady state response of load current before compensation (c) Steady state response of source current after compensation (d) Transient response of load current before compensation (e) Transient response of source current after compensation (f) Load voltage after compensation (g) DC-link voltage (h) Three phase compensating voltage for proposed controller based HSAPF system

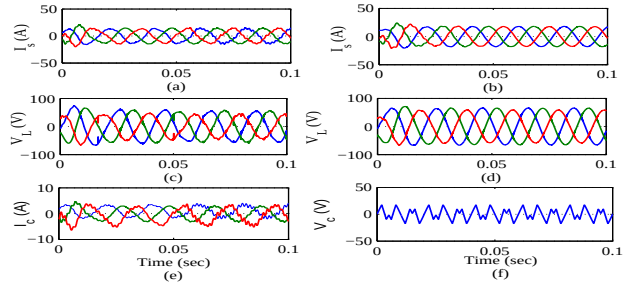

Fig. 8: (a) Three phase source current after compensation for existing controller based HSAPF (b) Three phase source current after compensation for proposed controller based HSAPF(c) Three phase load voltage after compensation for existing controller based HSAPF (d) Three phase load voltage after compensation for proposed controller based HSAPF (e) Three phase compensating current (f) Compensating voltage for phase-a in parametric variation case of HSAPF system

switching frequency to make the system more robust and stable but it produces more switching loss, chattering and white gaussian noise. But in case of proposed approach, sliding mode controller-2 is employed as voltage controller i.e. for switching pattern generation and HSRF method for reference voltage generation in HSAPF. The experimental studies for both steady state and dynamic conditions are performed and discussed in the following sections.

CASE-1: Balanced supply voltages with steady-state load condition:

The performance of the proposed HSAPF is verified through load impedance in initial case. A diode bridge rectifier with a R-L load is selected as the test load to measure the operation of HSAPF for load compensation.

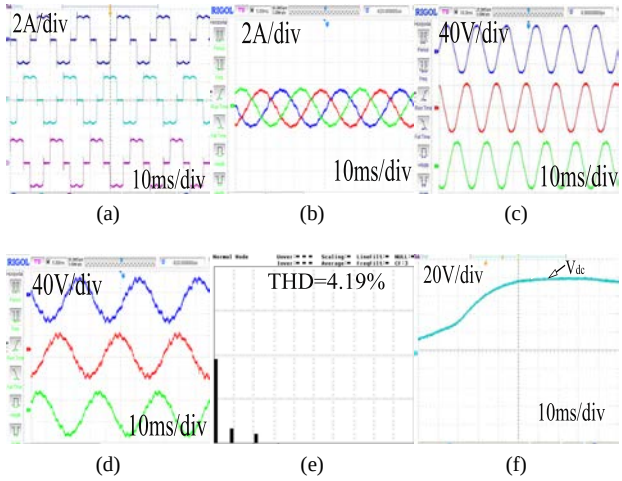

Fig. 9: Case-1a: (a) Three phase load current before compensation (b) Three phase source current after compensation (c) Three phase load voltage before compensation (d) Three phase load voltage after compensation (e) THD of source current after compensation (f) DC-link voltage in the existing method

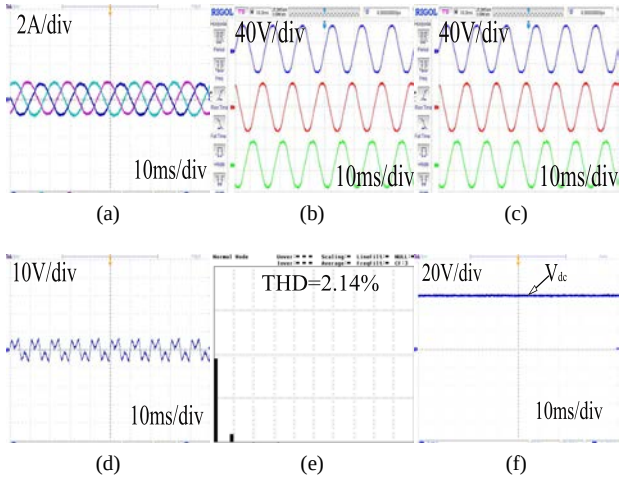

Fig. 10: Case-1b: (a) Three phase source current after compensation (b) Three phase load voltage before compensation (c) Three phase load voltage after compensation (d) Compensating voltage for phase-a (e) THD of source current after compensation (f) DC-link voltage in the proposed method

The three phase load currents (I_{La}, I_{Lb}, I_{Lc}) before compensation are shown in Fig. 9a. The source current is found to be sinusoidal. The source current, load voltage and the reference tracking behaviour of the compensating voltage for both the existing and proposed method has been presented in Fig. 9 and Fig. 10 respectively.

CASE-2: Balanced supply voltages with steady-state load condition as well as changing HSAPF parameters:

In this case, the HSAPF parameters are changed from $C_f = 50\mu$ F , $L_f = 0.35mH$ to $C_f = 60\mu$ F, $L_f = 1.35mH$. Under this condition, the performance of the proposed controller has been verified with existing method through Fig. 12 and Fig. 11. It is seen that in case of the proposed approach the source current are smooth

This article has been accepted for publication in a future issue of this journal, but has not been fully edited. Content may change prior to final publication. Citation information: DOI 10.1109/TPEL.2016.2586525, IEEE Transactions on Power Electronics

TABLE II: HARMONICS COMPENSATION EFFECT OF THE PROPOSED AND EXISTING CONTROL STRATEGY IN HSAPF(EXPERIMENTAL)

Cases	THD % phase-a source current			HCR (%)
	Methods used in HSAPF	Before comp. THD (%)	After comp. THD (%)	
Case-1	Proposed method	24.5	2.14	8.73
	Exist method	24.5	4.19	17.1
Case-2	Proposed method	20.14	1.6	7.94
	Exist method	20.14	4.16	20.65
Case-3	Proposed method	25.9	2.16	8.33
	Exist method	25.9	3.25	12.54
Case-4	Proposed method	26.7	2.16	8.08
	Exist method	26.7	3.25	12.17

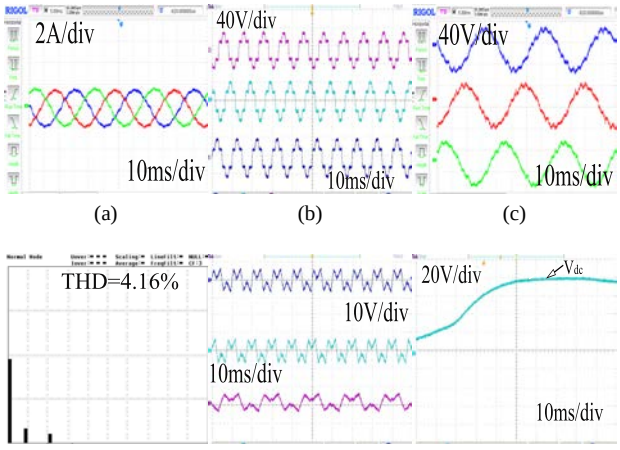

Fig. 11: Case-2a:(a) Three phase source current after compensation (b) Load voltage before compensation (c) Load voltage after compensation (d) THD of source current after compensation (e) Three phase compensating voltage (f) DC-link voltage in the exist method(ideal sliding mode controller)

and distortion less as compared to the existing method. Hence, the effective harmonic compensation is more in case of proposed method. Also the THD response of source current after compensation is superior in case of proposed method over existing method.

CASE-3: Balanced supply voltages with dynamic load condition:

The performance of the proposed HSAPF, assuming the balanced supply voltages, during a sudden load

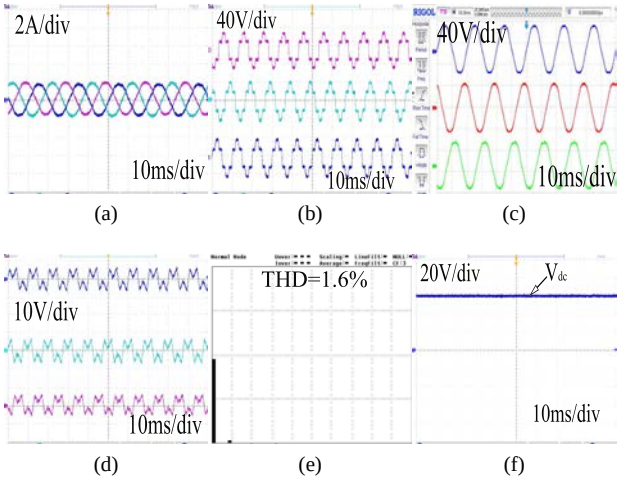

Fig. 12: Case-2b:(a) Three phase source current after compensation (b) Three phase load voltage before compensation (c) Three phase load voltage after compensation (d) Three phase compensating voltage (e) THD of source current after compensation (f) DC-link voltage for proposed method

varying condition is illustrated in Fig. 13 and Fig. 14. To create dynamic condition, the load is changed from ($R = 100\Omega$, $L = 40mH$) to ($R = 20\Omega$, $L = 10mH$). When the load change occurs, the compensating voltage quickly respond to changes to compensate the harmonic voltage and current in the load, as shown in Fig. 13. Also, the compensated source current can be viewed from Fig. 14a and Fig. 13b for both existing and proposed methods. As noticed, the HSAPF system with proposed approach achieves better performances in comparison to existing one. Furthermore, the dc link voltage in case of existing method settles to the reference value with a time delay of 0.1s, while a delay of only 0.024s is possible for the proposed technique as illustrated in Fig. 13d and Fig. 14c. Fig. 13 and Fig. 14 shows that the source current THD is effectively reduced from 25.9% to 2.16% and 3.25% in the proposed and existing method, respectively. Therefore this transient event demonstrates the actual capability and enhance the performance of the proposed approach over existing approach.

CASE-4: Unbalanced supply voltages with steady-state load condition:

In the previous cases, the supply voltages has been considered as sinusoidal and balanced, but this voltage is considered as unbalanced in nature. To verify the effectiveness of the proposed control algorithm under such condition, experiments have been carried out. The profiles for three phase supply voltages and source currents are shown in Fig. 15 and Fig. 16 respectively. This Fig. 16 shows that, the harmonic compensation performance of HSAPF has not deteriorated at unbalanced source voltage condition and the source currents are also balanced. But, a small no. of flickers are observed

This article has been accepted for publication in a future issue of this journal, but has not been fully edited. Content may change prior to final publication. Citation information: DOI 10.1109/TPEL.2016.2586525, IEEE Transactions on Power Electronics

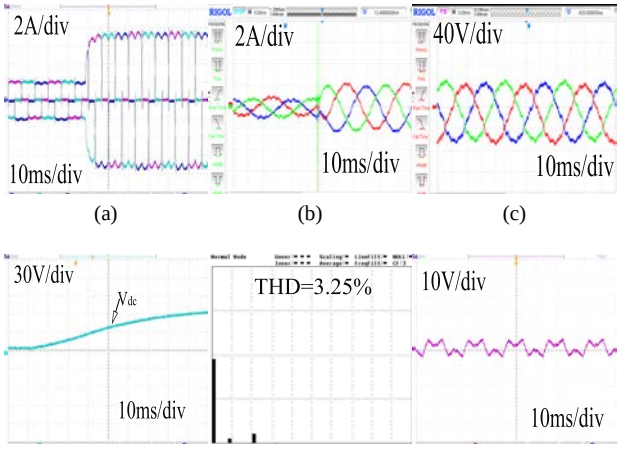

Fig. 13: Case-3a: (a) three phase load current before compensation (b) three phase source current after compensation (c) three phase load voltage after compensation (d) dc-link voltage (e) THD of source current after compensation (f) compensating voltage for phase-a

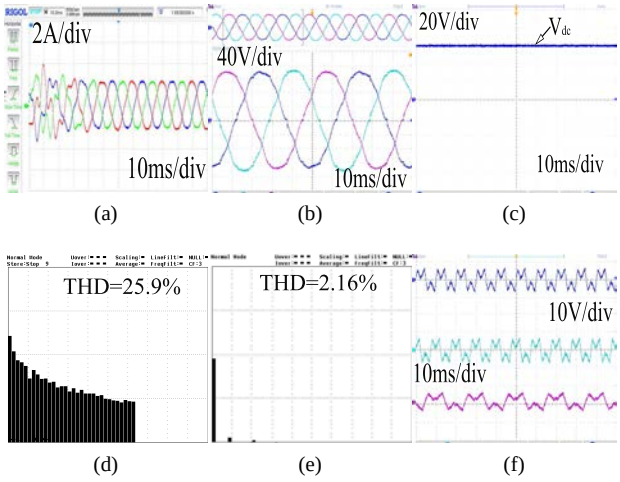

Fig. 14: Case-3b: (a) Three phase source current after compensation (b) Three phase load voltage after compensation (c) DC-link voltage (d) THD of source current before compensation (e) THD of source current after compensation (f) Three phase compensating voltage after compensation in the proposed method

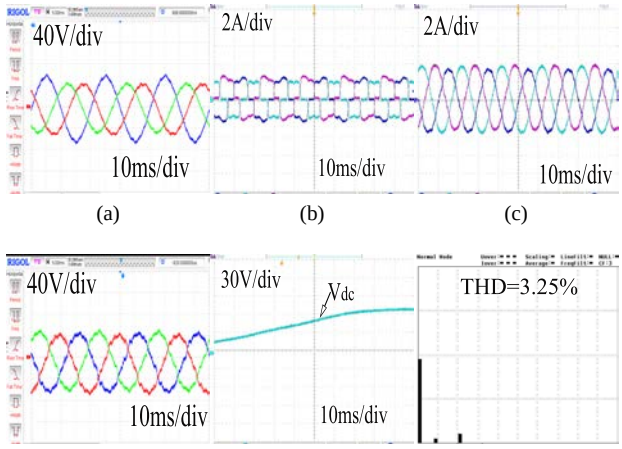

Fig. 15: Case-4a: (a) Three phase source voltage before compensation (b) Three phase load current before compensation (c) Three phase source current after compensation (d) Three phase load voltage after compensation (e) DC link voltage (f) THD of source current after compensation

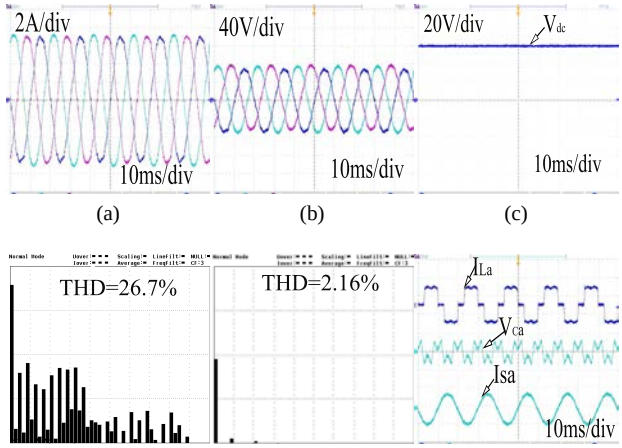

Fig. 16: Case-4b: (a) Three phase source current after compensation (b) Three phase load voltage after compensation (c) DC-link voltage (d) THD of source current before compensation (e) THD of source current after compensation (f) Compensating voltage with load current and source current after compensation in the proposed method

in case of existing method. THD analysis for phase-a supply current shown in Fig. 15 and Fig. 16, the proposed method has lower down the THD (i.e.2.16%) as compared to existing method (i.e. 3.25%) whereas the load current is distorted with a THD factor of 26.7%.

It is verified through experiments that the proposed controller based HSAPF has better steady state performances as well as better dynamic responses as compared to existing approach. In addition, to evaluate the robustness performance of the existing controller and the proposed controller assuming previously mentioned four cases, HCR factors are calculated and summarized in Table. II. The results of Table. II demonstrate that in case of proposed approach, HCR factors are maintained nearly the same i.e. 8% and these factors are unaffected by any perturbations raised in load or source sides, such robustness can not be achieved by using existing control strategy, in which HCR factor has been largely deviated in the presence of steady state and parametric variation behaviour of the load. Thus, the superiority of the proposed algorithm over existing method has been highlighted through all situations of power system perturbations.

VI. Conclusions

In this paper, a new robust controller design for HSAPF has been presented. The control design is established by sliding mode controller-2 that derives the equivalent control law. This control law is very much helpful for switching pattern generation. The robust-

ness of the proposed controller has been verified by analyzing the performance under steady state as well as transient condition of the power system. With the application of this technique, the functionalities of the HSAPF are enhanced. From the obtained simulations as well as experimental results, the proposed HSAPF has been observed to provide efficient current as well as voltage harmonic mitigation, reference voltage tracking behaviour, and reactive power compensation with dynamically varying load conditions. In the presence of an additive white noise, switching losses and distortion in both source current as well as load voltage, SRF method is found to be the best one for reference generation. Furthermore, the main feature of sliding mode controller-2 is the variable structure control method , which reduces tracking error distortion, suppress chattering, noise and hence a perfect gain stability of the HSAPF system has been achieved. The proposed filter can compensate source currents and also adjust itself to compensate for variations in non-linear load currents, maintain dc-link voltage at steady state and helps in the correction of power factor of the supply side adjacent to unity. Simulation and experimental results under several system operating conditions of load has verified the design concept of the suggested sliding mode based HSAPF to be highly effective and robust.

REFERENCES

[1] Z. Zeng, H. Yang, S. Tang, and R. Zhao, "Objective-oriented power quality compensation of multifunctional grid-tied inverters and its application in microgrids," *Power Electronics, IEEE Transactions on*, vol. 30, no. 3, pp. 1255–1265, 2015.

[2] A. B. Nassif, W. Xu, and W. Freitas, "An investigation on the selection of filter topologies for passive filter applications," *Power Delivery, IEEE Transactions on*, vol. 24, no. 3, pp. 1710–1718, 2009.

[3] M. Ali, E. Laboure, and F. Costa, "Integrated active filter for differential-mode noise suppression," *Power Electronics, IEEE Transactions on*, vol. 29, no. 3, pp. 1053–1057, 2014.

[4] E. R. Ribeiro and I. Barbi, "Harmonic voltage reduction using a series active filter under different load conditions," *Power Electronics, IEEE Transactions on*, vol. 21, no. 5, pp. 1394–1402, 2006.

[5] F. Z. Peng, H. Akagi, and A. Nabae, "A new approach to harmonic compensation in power systems-a combined system of shunt passive and series active filters," *Industry Applications, IEEE Transactions on*, vol. 26, no. 6, pp. 983–990, 1990.

[6] S. Diptimayee Swain, P. K. Ray, and K. Mohanty, "Voltage compensation and stability analysis of hybrid series active filter for harmonic components," in *India Conference (INDICON), 2013 Annual IEEE*, pp. 1–6, IEEE, 2013.

[7] W. Tangtheerajaroonwong, T. Hatada, K. Wada, and H. Akagi, "Design and performance of a transformerless shunt hybrid filter integrated into a three-phase diode rectifier," *Power Electronics, IEEE Transactions on*, vol. 22, no. 5, pp. 1882–1889, 2007.

[8] W. Guo, J. Wu, and D. Xu, "A novel sliding mode control of a high-voltage transformerless hybrid shunt active power filter," in *Industrial Electronics and Applications, 2009. ICIEA 2009. 4th IEEE Conference on*, pp. 2908–2913, IEEE, 2009.

[9] B. Kedjar and K. Al-Haddad, "Dsp-based implementation of an lqr with integral action for a three-phase three-wire shunt active power filter," *Industrial Electronics, IEEE Transactions on*, vol. 56, no. 8, pp. 2821–2828, 2009.

[10] R. Panigrahi, B. Subudhi, and P. C. Panda, "A robust lqg servo control strategy of shunt-active power filter for power quality enhancement," *Power Electronics, IEEE Transactions on*, vol. 31, no. 4, pp. 2860–2869, 2016.

[11] L. M. Fridman, "Singularly perturbed analysis of chattering in relay control systems," *IEEE Transactions on Automatic Control*, vol. 47, no. 12, pp. 2079–2084, 2002.

[12] M. A. Mulla, R. Chudamani, and A. Chowdhury, "A novel control method for series hybrid active power filter working under unbalanced supply conditions," *International Journal of Electrical Power & Energy Systems*, vol. 64, pp. 328–339, 2015.

[13] S. Rahmani, K. Al-Haddad, and H. Y. Kanaan, "Average modeling and hybrid control of a three-phase series hybrid power filter," in *Industrial Electronics, 2006 IEEE International Symposium on*, vol. 2, pp. 919–924, IEEE, 2006.

[14] S. D. Swain and P. K. Ray, "Harmonic current and voltage compensation using hsapf based on hybrid control approach for synchronous reference frame method," *International Journal of Electrical Power & Energy Systems*, vol. 75, pp. 83–90, 2016.

[15] H. De Battista and R. J. Mantz, "Harmonic series compensators in power systems: their control via sliding mode," *Control Systems Technology, IEEE Transactions on*, vol. 8, no. 6, pp. 939–947, 2000.

Sushree Diptimayee Swain pursuing Ph.D. degree in the Department of Electrical Engineering at National Institute of Technology (NIT) Rourkela, Rourkela. Her research is focused on application of non-linear control in power electronics.

Pravat Kumar Ray $(M'13)$ received the Ph.D. degree in electrical engineering from the National Institute of Technology (NIT) Rourkela, India, in 2011. He is currently an Assistant Professor with the Department of Electrical Engineering, NIT Rourkela.

His research interests include power system, power quality, solar irradiance forecasting using sky images and grid integration of renewable energy systems.

Kanungo Barada Mohanty received B. Tech. degree in Electrical Engineering from VSSUT, Burla in the year 1989. His M. Tech. and Ph.D. degrees are from IIT Kharagpur in the years 1990 and 2002, respectively. He is a faculty member of NIT Rourkela since 1991, and presently working as Associate Professor. He is Member of IEEE since 2008 and Senior Member of IEEE since February 2011. He is also Fellow of Institution of Engineers (India) and IETE. His research interests include vector control and direct torque control of induction machines, wind and solar energy systems, micro-grids.